

1

---

## 2 **Does it have to be Carbon? Metal Anodes in Microbial Fuel** 3 **Cells and related Bioelectrochemical Systems**

---

4

### 5 **SUPPORTING INFORMATION**

6

#### 7 **Preparation of Metal plated graphite electrodes (MPG electrodes)**

8 The manufacturing details were as follows: Silver powder (5  $\mu\text{m}$  – 8  $\mu\text{m}$ ,  $\geq$  99.9% trace metals  
9 basis) and copper powder (< 425  $\mu\text{m}$ , 99.5% trace metals basis) were purchased from Sigma-  
10 Aldrich. Nickel powder was precipitated from  $\text{NiCl}_2 \cdot 6 \text{H}_2\text{O}$  (Fluka >98%)<sup>21</sup> and gold powder was  
11 precipitated from  $\text{AuCl}_3$  in aqueous solution with hydrazine hydrate (Merck 99%). Graphite plates  
12 (CP Graphite GmbH, Germany) were cut into pieces of 10 mm x 10 mm and were polished by  
13 rubbing the surface over a sheet of paper. The respective metal powder was transferred into an  
14  $\text{Al}_2\text{O}_3$  crucible. This was placed in a vacuum vaporizer device (Mini Spectros, Kurt j. Lesker, USA),  
15 set at a pressure of  $5 \times 10^{-7}$  mbar. Now, the crucible was heated until a deposition of 40 nm metal  
16 was archived with a deposition rate of  $0.1 \text{ nm s}^{-1}$ . The samples were flushed with argon and were  
17 removed from the device.

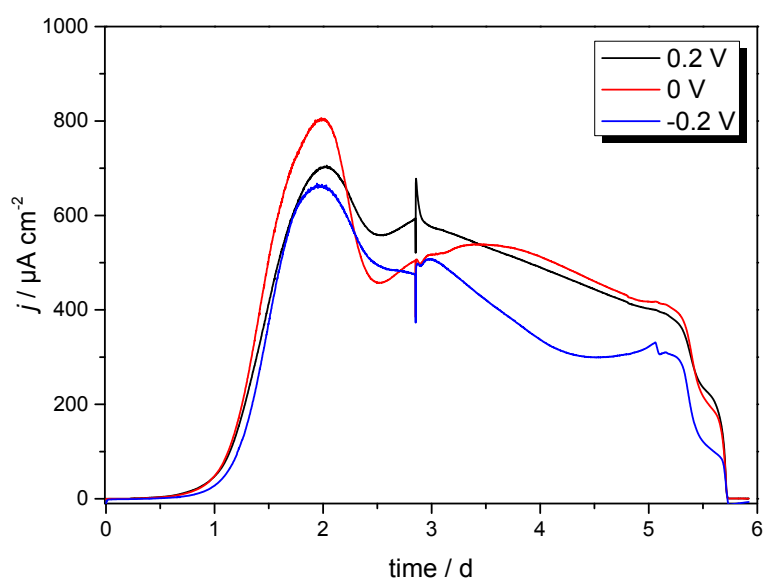
18

19 **Figure S1:** Exemplary scheme of the preparation of metal plated graphite electrodes (here: gold electrode).  
20 Electrode billet (left), gold plated electrode (center), and electrode connected via stainless steel wire  
21 (right).

22

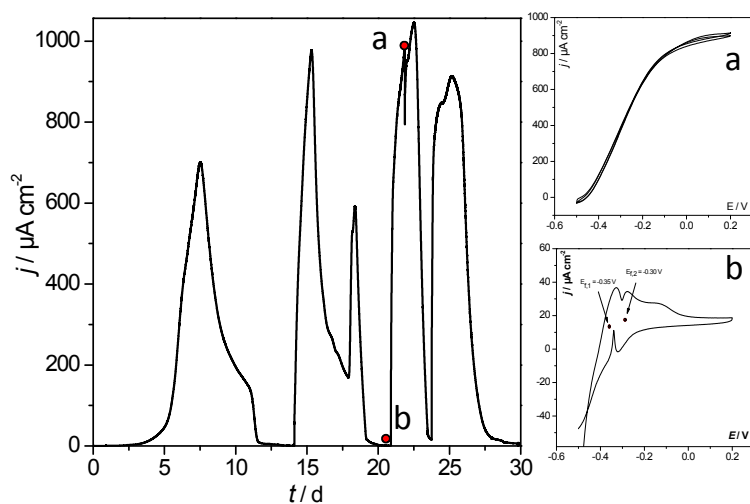
23 Each metalized graphite plate was connected via a stainless steel wire. A hole ( $d = 1.2 \text{ mm}$ ) was  
24 drilled 0.5 cm deep into the graphite plate. The end of the stainless steel wire ( $d = 0.6 \text{ mm}$ ) was  
25 folded to a double layer and squeezed into the hole leading to a stable mechanical connection and  
26 a high conductivity. Here, the immersion of conductive silver paint (Busch silver paint, Busch  
27 GmbH & Co. KG, Germany) into the hole improves the conductivity of the connection. All sides of  
28 the electrode except the metalized surface were insulated by applying a two-component non-  
29 conductive epoxy resin ("5 min Epoxy", R & G Faserverbundwerkstoffe, Germany). In a final step  
30 the stainless steel wire was insulated with a heat shrinking tube (Figure S1).

31  
 32  
 33 **Dependence of the biofilm formation and the biocatalytic electrode performance on the applied**  
 34 **electrode potential**

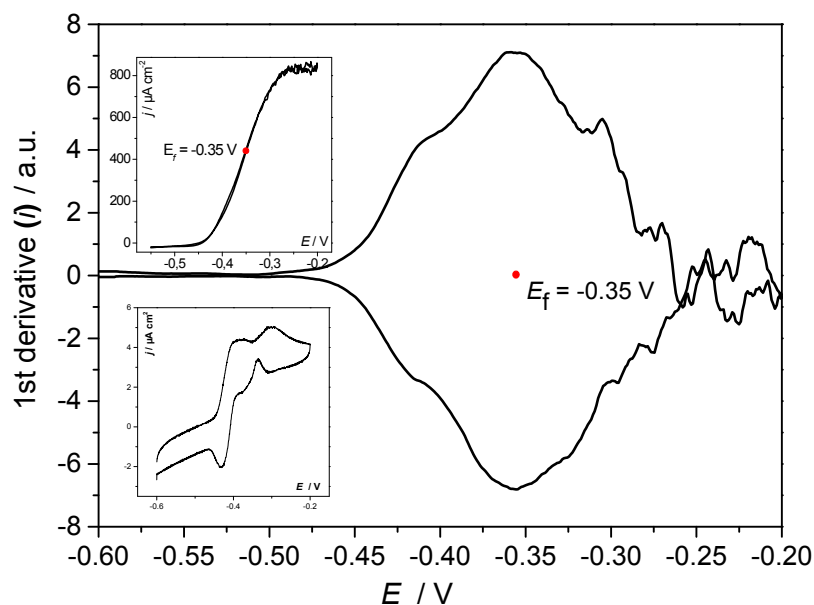


35  
 36 **Figure S2:** Exemplary cultivation and the resulting bioelectrocatalytic current generation of a secondary,  
 37 acetate based electrochemically active biofilm at a gold electrode in a batch experiment. The biofilm was  
 38 cultivated in a half-cell setup under potentiostatic control. The electrode potential was set at constant -0.2,  
 39 0 and +0.2 V (vs. Ag/AgCl).  
 40

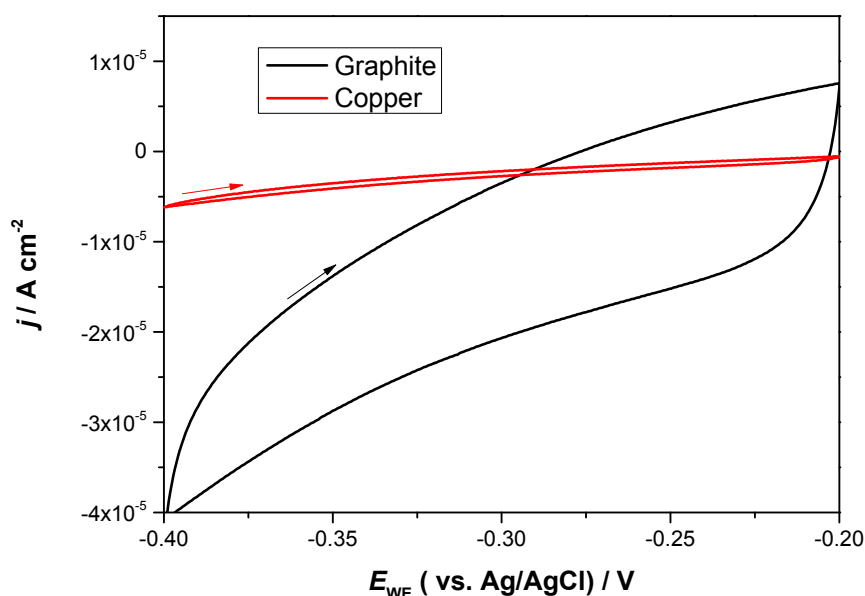
41 **Cyclic voltammetry of electrochemically active biofilms**



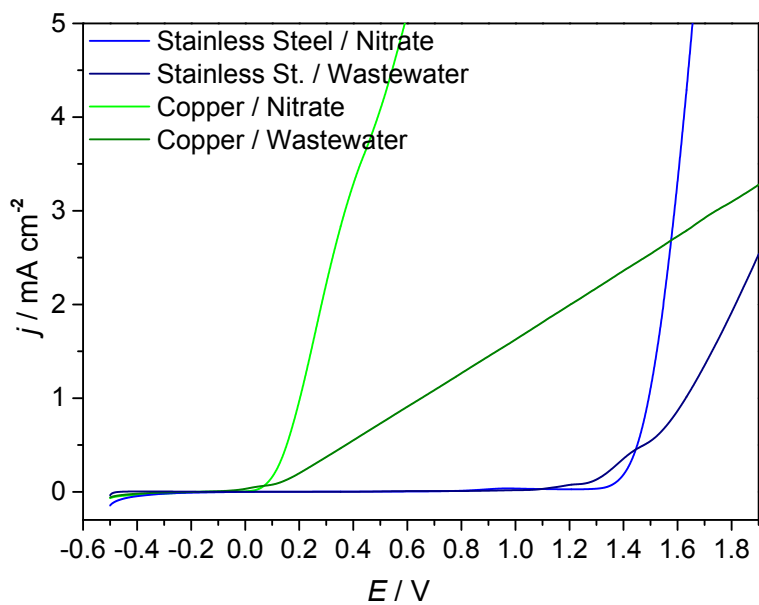
42  
 43 **Figure S3. Main Figure:** Exemplary cultivation and resulting bioelectrocatalytic current generation of a  
 44 **secondary**, acetate based electrochemically active biofilm at polycrystalline graphite in a semi-batch  
 45 experiment. The biofilm was cultivated in a half-cell setup under potentiostatic control. The electrode  
 46 potential was 0.2 V (vs. Ag/AgCl). Right figure column: **a:** cyclic voltammogram recorded under turnover  
 47 conditions (depicted by the red dot indexed “a” in the main figure). **b:** cyclic voltammogram recorded under  
 48 non-turnover conditions (depicted by the red dot indexed “b” in the main figure).



49  
 50 **Figure S4:** Cyclic voltammogram of a secondary, acetate based electrochemically active biofilm at a copper  
 51 electrode, recorded under turn-over conditions (upper inset figure) and the corresponding first derivative  
 52 of the voltammetric curve over the potential (main figure). The lower inset figure depicts a cyclic  
 53 voltammogram recorded under non-turnover-conditions.  
 54  
 55 **Voltammetric behaviour of selected electrode materials in the absence of a microbial biofilm**



56  
 57 **Figure S5.** Comparison of the cyclic voltammograms of copper and graphite in sterile bacterial growth  
 58 medium ("artificial wastewater"). The scan rate was  $10 \text{ mV s}^{-1}$ . No voltammetric/redox features of the  
 59 electrode materials or of the growth medium are visible. The polycrystalline graphite electrode exhibits  
 60 significantly larger capacitive currents than copper due to its porous structure.  
 61



62  
 63 **Figure S6.** Oxidative linear sweep voltammograms of blank copper and stainless steel (metal sheets),  
 64 recorded in 0.1 M potassium nitrate solution, as well as in filtrated primary wastewater (Scan rate 1 mV s<sup>-1</sup>.  
 65 The wastewater had a pH of 7 and a conductivity of 1.21 mScm<sup>-1</sup>.  
 66